DR DANIEL CHRISTOPHER NACHUN (Orcid ID : 0000-0002-0271-1135)
DR STEVE HORVATH (Orcid ID : 0000-0002-4110-3589)

Article type : Original Paper

Author Manuscript

Title: Clonal hematopoiesis associated with epigenetic aging and clinical outcomes

Author list: Daniel Nachun[1], Ake Lu[2], Alexander G. Bick[3,4], Pradeep Natarajan[3,4], Joshua Weinstock[5], Mindy D. Szeto[6], Sekar Kathiresan[3,4], Goncalo Abecasis[5], Kent D. Taylor[7], Xiuqing Guo[7], Russ Tracy[8], Peter Durda[8], Yongmei Liu[9], Craig Johnson[10], Steve S. Rich[11], David Van Den Berg[12], Cecilia Laurie[10], Tom Blackwell[5], George J. Papanicolaou[13], Adolfo Correa[14], Laura Raffield[15], Andrew Johnson[16], Joanne Murabito[17], JoAnn E. Manson[18], Pinkal Desai[19], Charles Kooperberg[20], Themistocles L. Assimes[21], Daniel Levy[16], Jerome I. Rotter[7], Alex P. Reiner[22], Eric Whitsel[23], James G. Wilson[24,25], Steve Horvath[2], Siddhartha Jaiswal[1,26,#] on behalf of the NHLBI Trans-Omics for Precision Medicine (TOPMed) Consortium

Corresponding author (sjaiswal@stanford.edu)

[1]Department of Pathology, Stanford University School of Medicine, Stanford, CA 94305
[2]Department of Human Genetics, David Geffen School of Medicine, University of California Los Angeles, Los Angeles, CA 90095
[3]Department of Medicine, Massachusetts General Hospital, Boston MA, 02114
[4]Broad Institute, Cambridge MA 02142
[5]Department of Biostatistics, University of Michigan School of Public Health, Ann Arbor MI 48109
[6]Division of Biomedical Informatics and Personalized Medicine, Department of Medicine, University of Colorado Anschutz Medical Campus, Aurora, CO 80045
[7]The Institute for Translational Genomics and Population Sciences, Department of Pediatrics, The Lundquist Institute for Biomedical Innovation at Harbor-UCLA Medical Center, Torrance, CA USA
[8]Department of Pathology and Laboratory Medicine, Larner College of Medicine, University of Vermont, Burlington, VT 05405
[9]Department of Medicine, Duke University Medical Center, Durham, NC 27710
[10]Department of Biostatistics, School of Public Health, University of Washington, Seattle, WA 98195

This is the author manuscript accepted for publication and has undergone full peer review but has not been through the copyediting, typesetting, pagination and proofreading process, which may lead to differences between this version and the Version of Record. Please cite this article as doi: 10.1111/ACEL.13366

This article is protected by copyright. All rights reserved

Author Manuscript

[11]Department of Public Health Sciences, University of Virginia School of Medicine, Charlottesville, VA 22908
[12]Department of Clinical Preventative Medicine, Keck School of Medicine, University of Southern California, Los Angeles, CA 90033
[13]Division of Cardiovascular Sciences, National Heart, Lung, and Blood Institute, Bethesda, MD 20892
[14]Department of Medicine, University of Mississippi Medical Center, Jackson, MS 39216
[15]Department of Genetics, University of North Carolina School of Medicine, Chapel Hill, NC 27514
[16]National Heart Lung and Blood Institute, Framingham MA 01702
[17]Department of Medicine, Boston University School of Medicine, Boston, MA 02118
[18]Department of Medicine, Brigham and Women’s Hospital, Harvard Medical School, Boston, MA 02115
[19]Department of Hematology/Oncology, Joan & Sanford I. Weill Medical College of Cornell University, New York, NY 10065
[20]Public Health Sciences Division, Fred Hutchinson Cancer Research Center, Seattle, WA 98109
[21]Department of Medicine, Stanford University School of Medicine, Stanford, CA 94305
[22]Department of Epidemiology, School of Public Health, University of Washington, Seattle, WA 98195
[23]Department of Epidemiology, Gillings School of Global Public Health, University of North Carolina, Chapel Hill, NC 27514
[24]Department of Cardiology, Beth Israel Deaconess Medical Center, Boston, MA 02215
[25]Department of Physiology and Biophysics, University of Mississippi Medical Center, Jackson, MS 39216
[26]Institute for Stem Cell Biology and Regenerative Medicine, Stanford University School of Medicine, Stanford, CA 94305

Graphical Abstract

Clonal hematopoiesis of indeterminate potential (CHIP) and epigenetic age acceleration are two important aging phenomenon associated with adverse clinical outcomes. We found that mutations in most CHIP genes were associated with increased age acceleration in multiple epigenetic clocks. Individuals with CHIP and age acceleration had a greatly increased risk of mortalitiy and coronary heart disease compared to individuals with only CHIP or age acceleration.

Abstract

Clonal hematopoiesis of indeterminate potential (CHIP) is a common precursor state for blood cancers that most frequently occurs due to mutations in the DNA methylation modifying enzymes *DNMT3A* or *TET2*. We used DNA methylation array and whole genome sequencing data from four cohorts together comprising 5,522 persons to study the association between CHIP, epigenetic clocks, and health outcomes. CHIP was strongly associated with epigenetic age acceleration, defined as the residual after regressing epigenetic clock age on chronological age, in several clocks, ranging from 1.31 years (GrimAge, $p < 8.6 \times 10^{-7}$) to 3.08 years (EEAA, $p < 3.7 \times 10^{-18}$). Mutations in most CHIP genes except DNA-damage response genes were associated with increases in several measures of age acceleration. CHIP carriers with mutations in multiple genes had the largest increases in age acceleration and decreases in estimated telomere length. Finally, we found that ~40%

This article is protected by copyright. All rights reserved

of CHIP carriers had acceleration > 0 in both Hannum and GrimAge (referred to as AgeAccelHG+). This group was at high risk of all-cause mortality (hazard ratio 2.90, $p < 4.1 \times 10^{-8}$) and coronary heart disease (CHD) (hazard ratio 3.24, $p < 9.3 \times 10^{-6}$) compared to those who were CHIP-/AgeAccelHG-. In contrast, the other ~60% of CHIP carriers who were AgeAccelHG- were not at increased risk of these outcomes. In summary, CHIP is strongly linked to age acceleration in multiple clocks, and the combination of CHIP and epigenetic aging may be used to identify a population at high risk for adverse outcomes and who may be a target for clinical interventions.

Introduction

Aging is inextricably associated with an increase in the number of somatic mutations, and this process is believed to be central to the development of cancer *(Welch et al. 2012; Martincorena & Campbell 2015; Hoang et al. 2016; Blokzijl et al. 2016; Risques & Kennedy 2018)*. Clonal hematopoiesis of indeterminate potential (CHIP) *(Jaiswal et al. 2014)* is defined by the presence of a cancer-associated somatic mutation in the blood cells of people without a blood cancer or other known clonal disorder. CHIP originates when hematopoietic stem cells (HSCs) acquire a random mutation, usually in an epigenetic factor, that results in increased clone fitness *(Jaiswal & Ebert 2019)*. CHIP is strongly associated with age, and carriers of these mutations have increased risk for developing blood cancers, but also coronary heart disease and all-cause mortality *(Jaiswal et al. 2014; Jaiswal et al. 2017)*. In addition to age, CHIP has been found to occur at a higher prevalence in males *(Jaiswal et al. 2014)* and a lower prevalence in people of self-reported Hispanic and East Asian ancestry compared to Europeans *(Jaiswal et al. 2014; Bick et al. 2020)*. The association of CHIP and heart disease may result from enhanced inflammatory gene expression in mutant macrophages within atherosclerotic plaques *(Jaiswal et al. 2017; Fuster et al. 2017; Bick AG et al. 2020)*, demonstrating that at least some of these mutations cause dysfunction of immune cells and affect phenotypes apart from cancer.

The availability of DNA methylation data from large epidemiological cohorts has advanced our understanding of epigenetic aging in recent years. Several "methylation clocks" have been developed *(Horvath 2013; Hannum et al. 2013; Levine et al. 2018; Horvath et al. 2018; Lu, Quach, et al. 2019)* which use methylation state at a subset of CpGs to predict chronological age with high accuracy in healthy individuals. "Age acceleration" results when predicted methylation age is greater than chronological age and associates with increased risk of coronary heart disease *(Levine et al. 2018; Lu, Quach, et al. 2019; Perna et al. 2016)* and all-cause mortality *(Levine et al. 2018; Lu, Quach, et al. 2019, p.201; Marioni et al. 2015a; Chen et al. 2016; Christiansen et al. 2016; Perna et al. 2016)*. Similar to prior studies (Horvath & Raj 2018), we defined age acceleration as the residual of a linear model of a clock estimate regressed against chronological age. By definition, this measure is not correlated with chronological age and a positive (or negative) value indicates that the clock age is higher (or lower) than expected based on chronological age. The factors underlying epigenetic age acceleration are incompletely understood. Recent work has noted two distinct categories of epigenetic

This article is protected by copyright. All rights reserved

Author Manuscript

108 clocks, intrinsic and extrinsic, which are believed to capture different aspects of aging. Intrinsic aging is
109 independent of cell-type and may be partly driven by the number of times a cell has divided *(Lu et al. 2018)*,
110 while extrinsic aging, is associated with changes of cell-type composition in blood *(Horvath et al. 2016)*, and
111 may be influenced by environmental factors *(Levine et al. 2018; Lu, Quach, et al. 2019)*. The Horvath and
112 IEAA clocks reflect intrinsic aging, whereas the Hannum, EEAA, PhenoAge, and GrimAge clocks are
113 measures of extrinsic aging (Table 1). GrimAge and PhenoAge were also trained to be predictors of mortality
114 *(Levine et al. 2018; Lu, Quach, et al. 2019)*. In addition, several DNA methylation-based predictors of other
115 aging-related phenotypes have recently been developed to improve mortality prediction, such as surrogate
116 biomarkers for plasma protein levels (adrenomedullin, beta-2-microglobulin, cystatin C, leptin, plasminogen
117 activator inhibitor 1, tissue inhibitor matrix metalloproteinase 1) *(Lu, Quach, et al. 2019)*, smoking pack-years
118 *(Lu, Quach, et al. 2019)*, and telomere length *(Lu, Seeboth, et al. 2019)*.
119 We hypothesized that CHIP may be an acquired genetic factor associated with epigenetic age
120 acceleration. Here, we use whole genome sequencing (WGS) and DNA methylation array data from several
121 cohorts within the Trans-omics for Precision Medicine (TOPMed) program to test the hypothesis that CHIP is
122 linked to epigenetic age acceleration. We find that CHIP is strongly associated with age acceleration in several
123 clocks. We further assess whether there are gene-specific associations of CHIP with epigenetic age and
124 methylation-estimated telomere length. Finally, we test whether the combination of CHIP status and epigenetic
125 age can be used to identify the group at highest risk for adverse outcomes.
126
127 **Results**
128 **Association between CHIP and epigenetic age acceleration in several clocks**
129 We used WGS data obtained from whole blood DNA for several large cohorts within TOPMed, including the
130 Framingham Heart Study (FHS), the Jackson Heart Study (JHS), the Women's Health Initiative (WHI), and the
131 Multi-Ethnic Study of Atherosclerosis (MESA), to identify CHIP as previously described *(Bick et al. 2020)* (see
132 Table S1 for a demographic summary of cohorts). The populations assayed for methylation were an unbiased
133 selection from within FHS and JHS, while the WHI TOPMed samples were over-sampled for incident stroke
134 and venous thromboembolism. The BA23 subset of WHI was a coronary heart disease case/control study.
135 Importantly, the blood draw used for methylation array analysis was the same as that used for WGS in FHS,
136 JHS and MESA, and in WHI, only persons for whom the blood draw for the WGS was within three years of the
137 draw for methylation were included. After adjusting age acceleration residuals for sex, self-reported ancestry,
138 and cohort, 5,522 individuals, including 319 CHIP carriers, from the four cohorts were assessed for seven
139 different aging measures: DNAmAge (Horvath) *(Horvath 2013)*, DNAmHannum (Hannum) *(Hannum et al.
140 2013)*, DNAmPhenoAge (PhenoAge) *(Levine et al. 2018)*, DNAmSkinClock (SkinBloodClock) *(Horvath et al.
141 2018)*, DNAmGrimAge (GrimAge) *(Lu, Quach, et al. 2019)*, intrinsic epigenetic age acceleration (IEAA) *(Lu et
142 al. 2018)* and extrinsic epigenetic age acceleration (EEAA) *(Lu et al. 2018)*, and a methylation-based estimate

Author Manuscript

This article is protected by copyright. All rights reserved

143 of telomere length (DNAmTL) (see Methods). The effects of CHIP were assessed overall (any CHIP mutation),
144 as well as at the level of specific classes of CHIP mutations (see Methods).
145 Consistent with previous results, carriers of CHIP were significantly older than non-carriers (+7.23 ±
146 0.61 years, $p < 1.13 \times 10^{-31}$, Figure S1 and S2), and the prevalence of CHIP reached >20% in those over 80
147 years (Figure S1). We then tested whether age acceleration residuals from several clocks bore any association
148 to CHIP (Figure 1). Similar to the results of Robertson et al. *(Robertson et al. 2019)*, CHIP was most strongly
149 associated with intrinsic age acceleration (Horvath: 3.01 years, $p < 3.0 \times 10^{-25}$; IEAA: 2.92 years, $p < 9.3 \times 10^{-26}$).
150 Due to our larger sample size, we also observed strong associations between CHIP and extrinsic age
151 acceleration (Hannum clock: 2.71 years, $p < 1.8 \times 10^{-23}$; EEAA: 3.08 years, $p < 3.7 \times 10^{-18}$), as well as PhenoAge
152 (2.21 years, $p < 1.0 \times 10^{-8}$), SkinBloodClock (1.58 years, $p < 2.5 \times 10^{-13}$) and GrimAge (1.31 years, $p < 8.6 \times 10^{-7}$).
153 We also found that the number of driver mutations was associated with a step-wise increase in age
154 acceleration for several clocks, and this relationship was strongest for Hannum and EEAA (Table S2).
155 We also found modest associations between CHIP and several epigenetic surrogate markers of plasma
156 proteins as well as blood counts (Table S3A-S3B), and between clock estimates and variant allele fraction
157 (VAF), which is an approximation of clone size (Table S4). Methylation data can also be used to estimate a
158 surrogate marker of leukocyte telomere length, DNAmTL *(Lu, Seeboth, et al. 2019)*. CHIP was associated with
159 reduced predicted age-adjusted DNAmTL in CHIP overall (-0.06, $p < 1.2 \times 10^{-8}$), as well as several mutation
160 classes (Figure S3A). An increasing number of mutations was associated with a decrease in predicted
161 DNAmTL (2 mut. vs. 1: -0.174, $p < 8.0 \times 10^{-7}$; >2 mut. vs. 2: -0.404, $p < 1.1 \times 10^{-5}$, Figure S3B-C).

162 **Gene-specific associations of CHIP with epigenetic age acceleration**

163 CHIP most commonly occurs due to mutations in genes coding for the DNA methylation-altering
164 enzymes *DNMT3A* and *TET2*, but can also arise due to mutations in *ASXL1*, *JAK2*, splicing factors, and DNA-
165 damage response (DDR) genes. Accordingly, we examined the associations of mutations in specific CHIP
166 genes with age acceleration (Table 2). In all clocks, the direction of association for *DNMT3A* and *TET2*
167 mutations was the same, although those with *TET2* mutations had significantly greater age acceleration than
168 those with *DNMT3A* mutations for Hannum (2.10 years, $p < 0.0012$) and EEAA (2.32 years, $p < 0.0063$), but
169 not other clocks. We also performed differential methylation analysis to assess whether mutations in the DNA-
170 methylation modifying enzymes *DNMT3A* and *TET2* had divergent effects at the clock CpGs. Mutations in
171 both genes primarily resulted in hypomethylation although a small number of CpGs showed hypermethylation
172 in *TET2* (Figure S4A-B). We also observed at the clock CpGs that the M-values (a log transformed measure of
173 the percent methylation at each site) in persons with *DNMT3A* and *TET2* mutations were highly correlated
174 (Figure S4C), indicating that the methylation state of persons with the two mutations are largely similar, despite
175 their opposing enzymatic effects.
176 Persons with mutations in multiple genes had the largest increases in age acceleration across all clocks
177 except PhenoAge, consistent with our observation that age acceleration increases with number of mutations.

This article is protected by copyright. All rights reserved

Author Manuscript

178 Conversely, no increase in age acceleration was observed in persons with mutations in DDR genes (*TP53*,
179 *PPM1D, BRCC3*), which is consistent with the lack of association with age acceleration observed for the same
180 mutations in cancer tissue samples *(Horvath 2013)*. Although we had only 8 individuals with *JAK2* mutations in
181 our cohort, these mutations showed an exceptionally strong association for a single mutation in several clocks,
182 the most extreme example being PhenoAge (10.01 years, $p < 9.7 \times 10^{-6}$). The PhenoAge clock was trained to
183 predict a composite measure of mortality risk which includes several hematological variables such as white
184 blood cell count, white blood cell differential and several red blood cell parameters which may be abnormal in
185 myeloproliferative neoplasm, a hematological malignancy which is strongly associated with *JAK2* mutations.
186 CHIP overall was nominally associated with estimated pack-years of smoking (DNAmPACKYRS), but only
187 mutations in *ASXL1* were significantly associated with this measure in a gene-specific analysis (7.54 pack-
188 years, $p < 0.002$), a finding that is in accordance with a recent report *(Bolton et al. 2020)* (Table S3).

189 **Association of CHIP and epigenetic age acceleration with clinical outcomes**

190 Several previous studies have linked both CHIP *(Jaiswal et al. 2014; Jaiswal et al. 2017)* and age
191 acceleration in some clocks *(Levine et al. 2018; Lu, Quach, et al. 2019)* to increased risk of adverse clinical
192 outcomes, in particular all-cause mortality and coronary heart disease (CHD). We asked whether the
193 combination of CHIP and age acceleration could further stratify carriers of CHIP into high-risk and low-risk
194 groups for these outcomes using Cox proportional hazards models adjusted for chronological age at blood
195 draw, low-density lipoprotein cholesterol, high-density lipoprotein cholesterol, triglycerides, systolic blood
196 pressure, type 2 diabetes status, smoking status, and self-reported ancestry in 4,088 persons from JHS, FHS,
197 and WHI (Figure 2B-C). In FHS, JHS, and WHI EMPC, which are unselected for CHD, there were 720 deaths
198 (74 in CHIP carriers) out of 3,624 participants (213 CHIP carriers) and 212 cases of incident CHD (22 in CHIP
199 carriers) out of 3,331 participants (192 CHIP carriers) after excluding those with CHD prevalent to time of blood
200 draw. In WHI BA23, which was a case-control study for CHD, there were 168 cases of incident CHD (18 in
201 CHIP carriers) in 458 total participants (42 CHIP carriers).

202 We defined a person to have 'age acceleration' (AgeAccel) for a clock if their values for an age
203 acceleration residual exceeded zero after adjustment for age at blood draw, sex, self-reported ancestry, and
204 study cohort. We then tested the interaction between this dichotomous variable and CHIP status in predicting
205 mortality in each of the seven clocks using Cox models. As shown in Table S5, we found that the most
206 significant interactions were for the Hannum and GrimAge clocks, although neither reached Bonferroni-
207 corrected statistical significance. Though both the Hannum and GrimAge clocks were predictive of time to
208 death or CHD in previous studies *(Lu, Quach, et al. 2019; Perna et al. 2016; Marioni et al. 2015b)*, they were
209 trained on different outcomes (age for Hannum versus time to death for GrimAge), and are not strongly
210 correlated in our dataset (bicor = **0.242**, $R^2 = 0.058$, Figure 2A). Therefore, we reasoned that a combined
211 measure incorporating age acceleration in *both* Hannum and GrimAge would better stratify high and low risk
212 groups because each clock provides orthogonal information. By this combined measure (henceforth referred

This article is protected by copyright. All rights reserved

Author Manuscript

to as AgeAccelHG), 102/255 (40%) of CHIP carriers were AgeAccelHG+ (age acceleration residual > 0 for both Hannum and GrimAge), compared to 922/3833 (24%) persons without CHIP. Considered individually in separate models, CHIP and AgeAccelHG were each associated with a modest increase in risk of all-cause mortality (CHIP: HR **1.27**, $p < 0.077$; AgeAccelHG: HR **1.84**, $p < 4.0\text{x}10^{-14}$), consistent with previous findings. When we modeled the interaction of CHIP with AgeAccelHG for all-cause mortality, we found a significant interaction effect (CHIP main effect: coefficient = **-0.25**, $p < 0.20$; AgeAccelHG main effect: coefficient = **0.51**, $p < 3.08\text{x}10^{-9}$; interaction: coefficient = **0.80**, $p < 3.74\text{x}10^{-3}$), which remained significant after Bonferroni correction for eight tests.

To validate this finding, we sought replication in an independent cohort, the BA23 subset of WHI, which was not used in the above mortality analysis *(Horvath et al. 2016)*. When we modeled the interaction of CHIP with AgeAccelHG for CHD in BA23, the interaction term was again significant (CHIP main effect: coefficient = **-0.24**, $p < 0.60$; AgeAccelHG main effect: coefficient = **0.24**, $p < 0.35$; interaction: coefficient = **1.72**, $p < 0.01$).

Having demonstrated a significant statistical interaction between CHIP and AgeAccelHG for clinical outcomes, we combined these two variables into a single, 4-factor variable for further modeling. For CHD, we included incident events in FHS, JHS, and WHI EMPC together with WHI BA23 as a meta-analysis. Persons who were CHIP+/AgeAccelHG+ had much greater risk of all-cause mortality (HR **2.90**, $p < 4.1\text{x}10^{-8}$) and CHD (HR **3.24**, $p < 9.3\text{x}10^{-6}$) compared to those who were CHIP-/AgeAccelHG-. Those who were CHIP-/AgeAccelHG+ had a more modest increase in risk of all-cause mortality (HR **1.66**, $p < 3.1\text{x}10^{-9}$), and CHD (HR **1.39**, $p < 0.012$) compared to those who were CHIP-/AgeAccelHG-. In contrast, those who were CHIP+/AgeAccelHG- did not have elevated risk of either all-cause mortality (HR **0.78**, $p < 0.20$) or CHD (HR **1.03**, $p < 0.93$) compared to those who were CHIP-/AgeAccelHG- (Figure 2B-C). We also fitted contrasts to estimate the hazard ratios for all-cause mortality and CHD for CHIP only in persons with AgeAccelHG+ and AgeAccelHG+ only in persons with CHIP, in both cases finding the associations to be significant (Figure S5).

We also asked if there were gene-level differences in risk of these outcomes. We had insufficient sample size to assess either mortality or CHD individually, so we combined the two into a composite outcome. Being AgeAccelHG+ increased the risk of the composite outcome for those with *TET2* mutations relative to those who were CHIP-/AgeAccelHG- (*TET2* mutated+/AgeAccelHG+: HR = **3.88**, $p < 1.6\text{x}10^{-6}$; *TET2* mutated+/AgeAccelHG-: HR = **1.14**, $p < 0.66$; p for interaction < 0.065) to a greater degree than those with *DNMT3A* mutations (*DNMT3A* mutated+/AgeAccelHG+: HR = **1.99**, $p < 0.028$; *DNMT3A* mutated+/AgeAccelHG-: HR = **0.68**, $p < 0.079$; p for interaction < 0.11) or other non-DDR mutations (other mutation+/AgeAccelHG+: HR = **2.88**, $p < 1.1\text{x}10^{-5}$; other mutation+/AgeAccelHG-: HR = **1.00**, $p < 1$; p for interaction < 0.19).

To illustrate absolute risks among those with both CHIP and AgeAccelHG, we determined the cumulative incidence of all-cause mortality and CHD in persons from FHS, JHS, and WHI EMPC aged 65 or older at blood draw who did not have prevalent coronary heart disease (Figure 2D-E). Those who were

Author Manuscript

This article is protected by copyright. All rights reserved

CHIP+/AgeAccelHG+ had a cumulative incidence of all-cause mortality of 46.6% by 10 years and a cumulative incidence of CHD of 22.2% by 10 years. In contrast, the other three groups had substantially lower 10-year cumulative incidence of all-cause mortality (CHIP+/AgeAccelHG- 17.7%, CHIP-/AgeAccelHG+ 25.8%, CHIP-/AgeAccelHG- 19.2%) and CHD (CHIP+/AgeAccelHG- 7.98%, CHIP-/AgeAccelHG+ 13.0%, CHIP-/AgeAccelHG- 8.66%).

Our data permitted us to also ask whether there was an association of CHIP and AgeAccelHG to time to death in those who had a first CHD event, a subgroup that is often the target of clinical interventions. We restricted our analysis to individuals who had a first CHD event after age 70 and, if they died, did so more than 30 days after the CHD event. We found a significant interaction between CHIP and AgeAccelHG for all-cause mortality after CHD ($p < 0.036$). Persons who were CHIP+/AgeAccelHG+ showed significant increase in risk of all-cause mortality (HR = **3.16**, $p < 1.16\times10^{-5}$), while those who were CHIP+/AgeAccelHG- (HR = **0.462**, $p < 0.27$) or CHIP-/AgeAccelHG+ (HR = **1.40**, $p < 0.13$) showed no significant increase. The 5-year cumulative incidence of death after CHD for those who were CHIP+/AgeAccelHG+ was 58.5%, while for all other groups it was substantially lower (CHIP+/AgeAccelHG- 18.8%, CHIP-/AgeAccelHG+ 20.0%, CHIP-/AgeAccelHG- 19.8%, Figure 2F).

Given the previous findings linking both CHIP *(Jaiswal et al. 2017)* and extrinsic epigenetic aging *(Levine et al. 2018; Lu, Quach, et al. 2019; Horvath et al. 2016)* to inflammation, we asked whether plasma levels of the inflammation marker high-sensitivity C-reactive protein (hsCRP) showed any evidence of interaction with CHIP for all-cause mortality or CHD. We found evidence for a main effect of hsCRP on risk for all-cause mortality, but not for an interaction with CHIP (CHIP main effect: coefficient = **0.22**, $p < 0.22$; log(hsCRP) main effect: coefficient **= 0.09**, $p < 1.01\times10^{-3}$; interaction: coefficient = **0.076**, $p < 0.29$). For CHD, no effect of hsCRP was observed (CHIP main effect: coefficient = 0.23 $p < 0.49$; log(hsCRP) main effect: coefficient = **0.01**, $p < 0.90$; interaction: coefficient = **-0.3**, $p < 0.82$). We also stratified our cohort into 8 groups based upon CHIP status, AgeAccelHG status, and whether hsCRP levels were above 2 mg/L, an established clinical cutoff. Individuals with CHIP and AgeAccelHG showed a similar risk of all-cause mortality and CHD regardless of whether they had high or low hsCRP levels (Figure S5E-F). These results indicate that hsCRP is a poor discriminator of risk in CHIP carriers, unlike AgeAccelHG.

A coding SNP in *IL6R* (rs2228145), which results in Asp358Ala, was previously found to attenuate the increased risk for mortality and CHD associated with CHIP *(Bick AG et al. 2020)*. Here, the interaction between CHIP status and alternate allele count at rs2228145 was not significant for either all-cause mortality (CHIP main effect: coefficient = **0.27**, $p < 0.158$; rs2228145 main effect: coefficient = **-0.082** per alternate allele, $p < 0.21$; interaction: coefficient = **-0.044** per alternate allele, $p < 0.82$) or CHD (CHIP main effect: coefficient = **0.23**, $p < 0.36$; rs2228145 main effect: coefficient = **-0.16** per alternate allele, $p < 0.08$; interaction: coefficient = **0.25** per alternate allele, $p < 0.36$). There were also no significant interactions between rs2228145 genotype and the combined CHIP/AgeAccelHG variable (Figure S5C-D). These results indicate that *IL6R* genotype is a

Author Manuscript

This article is protected by copyright. All rights reserved

283 poor discriminator of risk in CHIP carriers in this dataset, unlike AgeAccelHG. However, we did find
284 differences based on which gene was mutated. Those who were *TET2*-CHIP+/AgeAccelHG+ and with no
285 alternate alleles of rs2228145 (*IL6R*WT) had the highest risk for the composite mortality/CHD outcome relative
286 to the referent group of CHIP-/AgeAccelHG-/*IL6R*WT (HR = **11.3**, $p < 2.4 \times 10^{-21}$, Figure S6). Those who were
287 *TET2*-CHIP+/AgeAccelHG+ but carried 1 or 2 alternate alleles of rs2228145 (*IL6R*Mut) had substantially lower
288 risk (HR = **1.91** compared to the same referent group, $p < 0.066$; coefficient for interaction = **-1.12** per alternate
289 allele, p for interaction < 9.6×10^{-7}, Figure S6). There was no significant difference in risk based on rs2228145
290 genotype in those who were *TET2*-CHIP+/AgeAccelHG-. We also did not find significant differences in risk of
291 death/CHD by rs2228145 genotype in *DNMT3A*-CHIP or CHIP with other non-DDR mutations regardless of
292 AgeAccelHG status.
293
294 **Discussion**
295 The results presented here permit us to draw several conclusions. First, it is clear that CHIP is strongly
296 associated with epigenetic aging in several clocks. Consistent with the results from Robertson et al. *(Robertson*
297 *et al. 2019)*, we find the strongest associations to be with the intrinsic clocks, Horvath and IEAA. This could
298 reflect a shared genetic architecture, as evidenced by the overlapping GWAS hits between polymorphisms
299 near *TERT* and *TRIM59* that associate with both CHIP and IEAA *(Bick et al. 2020; Zink et al. 2017)*. However,
300 the heritability of CHIP appears to be low (3.6% *(Bick et al. 2020)*), which limits our ability to test for genetic
301 correlation between CHIP and age acceleration. Previous studies have shown that IEAA of cultured
302 fibroblasts strongly correlates with the number of population doublings *(Lu et al. 2018)*. Therefore, an
303 alternative hypothesis is that the increase in intrinsic age acceleration seen in CHIP carriers may be due to
304 either 1) increased proliferation or self-renewal of HSC clones that harbor these mutations or 2) stem cell
305 exhaustion of wild-type HSCs from over-proliferation, leading to a selective advantage for mutant clones.
306 Studies in model systems such as genetically modified mice may help delineate the cause-effect relationship
307 between mutations in various CHIP-associated genes and intrinsic age acceleration.
308 Most importantly, our results show that it is possible to stratify CHIP carriers into those at high versus
309 low risk of adverse clinical outcomes using a composite measure of Hannum and GrimAge (AgeAccelHG).
310 CHIP or AgeAccelHG status alone is associated with a modestly increased risk of death or CHD, but the
311 combination of CHIP+ and AgeAccelHG+ is synergistic for these outcomes. Furthermore, CHIP in the absence
312 of epigenetic aging in these clocks is not associated with adverse outcomes. These results suggest that the
313 effects of CHIP on health are context dependent, as Hannum and GrimAge are not uniformly increased in all
314 CHIP carriers, and may be influenced by environmental factors such as CRP, smoking, diet, BMI, insulin
315 resistance, education level, exercise, socioeconomic status *(Quach et al. 2017)*, traumatic stress *(Wolf et al.*
316 *2018)*, insomnia *(Carroll et al. 2017)*, and hunter-gatherer lifestyle *(Horvath et al. 2016)*. Our results may also
317 explain why the strength of the associations between CHIP and mortality or CHD are somewhat inconsistent

Author Manuscript

This article is protected by copyright. All rights reserved

318 across studies—while the prevalence of CHIP is fairly uniform across populations, epigenetic aging may not
319 be. In populations with a high prevalence of risk factors for epigenetic aging, the consequences of CHIP may
320 be more dire than in populations without such risk factors.

321 Our risk stratification schema may also be used to select patients for clinical trials of pharmaceutical or
322 behavioral interventions, as the benefit-to-risk ratio may be particularly favorable in the high-risk CHIP group.
323 We note that that the 5-year mortality after CHD in those who are CHIP+ and AgeAccelHG+ approaches 60%,
324 similar to the mortality seen in patients with intermediate-risk MDS *(Greenberg et al. 2012)*. Furthermore, the
325 high event rate in this group would enable smaller trials with sufficient power for detecting favorable outcomes
326 such as reduced all-cause mortality or time to CHD. One such intervention may be blockade of IL-6 receptor
327 *(Bick AG et al. 2020)*; our results show that those who are *TET2*-CHIP+ and AgeAccelHG+ have lower risk of
328 death or CHD with increasing copies of rs2228145, which has previously been linked to reduced IL-6R
329 expression levels in myeloid cells *(Bick AG et al. 2020)*. Alternatively, this group may benefit from IL-1B
330 inflammatory blockade *(Ridker et al. 2017)*, which has also been shown to be relevant to atherosclerosis in
331 model systems of CHIP *(Jaiswal et al. 2017; Fuster et al. 2017)*. Of note, AgeAccelHG appears to be superior
332 to hs-CRP and genotype at *IL6R* for risk discrimination of CHIP carriers, implying that it is capturing additional
333 information beyond baseline inflammation.

334 In sum, our results show that there is an important relationship between CHIP and epigenetic aging.
335 CHIP and epigenetic age acceleration can also be used to identify persons at high risk of all-cause mortality
336 and CHD, further reinforcing the importance of both phenotypes as valuable tools in precision medicine for
337 aging.
338
339

340 **Methods**

341 *Epidemiological cohorts*

342 All participant data were obtained from four independent patient cohorts: the Framingham Heart Study (FHS)
343 *(Feinleib et al. 1975)*, the Jackson Heart Study (JHS) *(Sempos et al. 1999)*, the Women's Health Initiative
344 (WHI) (phs000200.v11.p3), and the Multi-ethnic Study of Atherosclerosis (MESA) *(Bild 2002, p.200)*. These
345 cohorts were included in the Trans-Omics for Precision Medicine (TOPMed) consortium which is run by the
346 National Heart Lung and Blood Institute of the National Institutes of Health. Access to all data was approved
347 by TOPMed as well as the individual cohorts. We included only those persons from these cohorts in which the
348 age at draw for both whole blood methylation and whole genome sequencing (WGS) were available. In the
349 FHS and JHS cohorts, the samples for methylation and WGS were taken from the same blood draw in all
350 persons. In MESA, methylation data was only used from the first exam as this was the time at which DNA for
351 WGS was also collected. In the WHI cohort, the two samples were often taken from different times. We only
352 considered persons for whom the methylation and WGS samples were taken within 3 years of each other.

Author Manuscript

This article is protected by copyright. All rights reserved

353

354 *Methylation array data*

355 Whole blood methylation was quantified using the Illumina MethylationEPIC or HumanMethylation450k array.
356 Normalized methylation data was submitted to the online methylation clock tool
357 (https://dnamage.genetics.ucla.edu/new) which generates methylation age estimates for seven different clocks:
358 DNAmAge *(Horvath 2013)*, DNAmHannum *(Hannum et al. 2013)*, DNAmPhenoAge *(Levine et al. 2018)*,
359 DNAmSkinClock *(Horvath et al. 2018)*, DNAmGrimAge *(Lu, Quach, et al. 2019)*, intrinsic epigenetic age
360 acceleration (IEAA) *(Lu et al. 2018)* and extrinsic epigenetic age acceleration (EEAA) *(Lu et al. 2018)*. Age
361 acceleration was computed for each measure as the residual of model predicting each persons' methylation
362 age from their chronological age at the time of blood draw. Additionally, the DNAmGrimAge clock generates
363 seven surrogate biomarkers based upon blood protein expression (MADM/NRBP1, B2M, CST3 (Cystatin C),
364 GDF15, LEP (Leptin), SERPINE1/PAI1, and TIMP1) as well smoking pack-years. Age-adjusted leukocyte
365 telomere length (LTL) and unadjusted LTL are also estimated by the clock software *(Lu, Seeboth, et al. 2019)*.
366 Cell composition was also estimated by the clock software using a published model *(Houseman et al. 2012)*.

367

368 *Identification of somatic variants*

369 Approximately 100,000 whole genomes were sequenced from whole blood DNA to ~30X depth as part of the
370 TOPMed study *(Bick et al. 2020)*. Somatic mutations associated with clonal hematopoiesis of indeterminate
371 potential (CHIP) were called from WGS data using the Mutect2 module in GATK from BAM files previously
372 aligned with BWA. Candidate CHIP variants were selected based upon a curated list of known variants
373 recurrently mutated in hematological malignancies as previously described *(Jaiswal et al. 2017)* (see Table
374 S6). A full list of variants identified in this study are included in Table S7.

375

376 *Association between CHIP and methylation age acceleration*

377 CHIP status was associated with age acceleration and the other measures using linear modeling, with a
378 separate model being fitted for each aging measure. Because of the relatively small number of comparisons,
379 p-values for these analyses were reported unadjusted. We combined the data from all three studies and used
380 residualization to remove the effects of age, race/ethnicity, sex, and study. This approach was chosen to
381 eliminate any possibility of spurious associations between CHIP and the methylation measures that were
382 driven by collinearity between CHIP and covariates. The residualized methylation measure was the outcome
383 in each model, and a likelihood ratio test was performed to test the significance of CHIP as predictor against a
384 null model containing only the intercept. When testing the association of CHIP mutations with specific genes,
385 CHIP status was replaced with a categorical variable indicating whether the individual had a mutation in that
386 gene, and persons with CHIP mutations in other genes were excluded. The following specific categories for
387 single mutations were used: *DNMT3A*, *TET2*, DNA damage response (DDR, which includes *TP53*, *PPM1D*,

This article is protected by copyright. All rights reserved

Author Manuscript

388 and *BRCC3*), *JAK2*, *ASXL1/2* (includes *ASXL1* and *ASXL2*), splicing factor (includes *SF3B1*, *SRSF2*, *U2AF1*,
389 *ZRSR2*, and *PRPF8*), and other for any single gene which did not fit in the previous categories. Persons with
390 mutations in more than one gene were classified as multiple regardless of the number of mutations or which
391 genes were mutated, while persons with multiple mutations in the same gene were classified as singletons.
392 The analysis of mutation number vs. methylation measures grouped all persons with single mutation into one
393 group, and split the group with mutations in multiple genes into 2 mutations and greater than 2 mutations,
394 regardless of which genes were mutated. Correlation between VAF and the residualized methylation measures
395 was computed using biweight midcorrelation, an outlier resistant alternative to Pearson's correlation *(Horvath*
396 *2011)*.
397
398 *Differential methylation of clock CpGs*
399 Illumina HumanMethylation450K and MethylationEPIC CpG probe IDs for the clocks and DNAmLTL were
400 obtained from the supplemental data of the relevant publications. Methylation beta values for each cohort
401 were subsetted for CpGs used in all clocks except GrimAge (for which the CpG locations have not been
402 published), and were converted to M-values. The M-values were adjusted for the same covariates that were
403 considered for the methylation clock measures. The adjusted residuals were tested for differential methylation
404 and p-values corrected for the number of CpGs tested using limma(Ritchie et al. 2015).
405
406 *Association of CHIP and epigenetic age acceleration with clinical outcomes*
407 We tested the associations of CHIP and epigenetic age acceleration with all-cause mortality and incident
408 coronary heart disease with Cox proportional hazards models using the *survival* package in R. Models
409 included age, sex, race/ethnicity, systolic blood pressure, type 2 diabetes status, plasma LDL-cholesterol
410 concentration, plasma HDL-cholesterol concentration, plasma triglyceride concentration, and smoking status
411 as covariates. Some persons in WHI had DNA for the methylation and/or WGS sample obtained several years
412 after the baseline visit, which potentially could introduce survivorship bias into the analysis. For this reason, we
413 also excluded anyone in WHI for whom either the methylation or WGS blood draw occurred more than 5 years
414 after the baseline visit.
415
416 For analysis of all-cause mortality, pooled data from FHS, JHS, and WHI EMPC were used. The selection of
417 samples used in TOPMed in these cohorts were taken essentially at random from the larger parent cohorts.
418 WHI BA23 was excluded from this analysis because persons in this cohort were over-sampled for CHD. MESA
419 was excluded from this analysis because persons in this cohort were selected for surviving at least 10 years
420 from baseline. We chose to present the results from models in which all three cohorts were pooled, rather than
421 analyzed separately and then meta-analyzed. The results for the meta-analysis were similar, however

Author Manuscript

This article is protected by copyright. All rights reserved

422 (CHIP/AgeAccelHG interaction pooled: coefficient = 0.80, $p < 3.7x10^{-3}$; CHIP/AgeAccelHG interaction in fixed
423 effects meta-analysis: coefficient = 0.85, $p < 2.4x10^{-3}$).
424
425 For the analysis of CHD, the WHI BA23 cohort was analyzed separately, and a meta-analysis was used to
426 combine the results of the BA23 analysis with the other pooled cohorts (JHS, FHS, and WHI EMPC) to get the
427 final effect size estimates. 45 persons in WHI BA23 were also included in the mortality analysis of WHI EMPC,
428 but were not included in the CHD analysis of WHI EMPC (i.e., were not double counted). Because BA23 was
429 oversampled for CHD, we adjusted the sample weights in BA23 using race and incident CHD numbers in the
430 entire dbGaP-eligible set of WHI to allow for Cox proportional hazards modeling. Robust standard errors were
431 used to calculate p-values in all models.
432
433 Similar to the associations between CHIP and age acceleration, p-values for these analyses were reported
434 unadjusted due to the small number of comparisons. We used the age acceleration residuals from the
435 analysis associating CHIP with epigenetic age acceleration to determine if persons had high age acceleration
436 (AgeAccelHG, defined as being greater than 0 for both AgeAccelHannum and AgeAccelGrim) and intersected
437 this with CHIP status, resulting in four groups: no CHIP with low age acceleration, no CHIP with high age
438 acceleration, CHIP with low age acceleration, and CHIP with high age acceleration. When we analyzed the
439 interaction of individual clocks with CHIP status, we used the same definition for age acceleration but restricted
440 it to only one clock.
441
442 For the gene-level analyses, persons with any singleton *DNMT3A*, *TET2*, or DDR gene (*TP53*, *PPM1D*,
443 *BRCC3*) mutation were considered to be in those classes. All other non-*DNMT3A*, *TET2* and DDR mutations
444 were considered "other". In those with multiple mutations, the mutated gene with the highest VAF was used to
445 assign the class.
446
447 For the analysis of cumulative incidence of death and CHD, the *cmprsk* package in R was used.
448

449 **Acknowledgements**

450 Whole genome sequencing (WGS) for the Trans-Omics in Precision Medicine (TOPMed) program was
451 supported by the National Heart, Lung and Blood Institute (NHLBI). WGS for "NHLBI TOPMed: Whole Genome
452 Sequencing and Related Phenotypes in the Framingham Heart Study" (phs000974.v1.p1) was performed at
453 the Broad Institute of MIT and Harvard (HHSN268201500014C). WGS for "NHLBI TOPMed: The Jackson
454 Heart Study" (phs000964.v1.p1) was performed at the University of Washington Northwest Genomics Center
455 (HHSN268201100037C). WGS for "NHLBI TOPMed: Multi-Ethnic Study of Atherosclerosis (phs001416.v1.p1)
456 was performed at the Broad Institute of MIT and Harvard (HHSN268201500014C). WGS for "NHLBI TOPMed:

This article is protected by copyright. All rights reserved

Author Manuscript

Women's Health Initiative (phs001237.v1.p1) was performed at the Broad Institute of MIT and Harvard (HHSN268201500014C). Centralized read mapping and genotype calling, along with variant quality metrics and filtering were provided by the TOPMed Informatics Research Center (3R01HL-117626-02S1; contract HHSN268201800002I). Phenotype harmonization, data management, sample-identity QC, and general study coordination were provided by the TOPMed Data Coordinating Center (3R01HL-120393-02S1; contract HHSN268201800001I). We gratefully acknowledge the studies and participants who provided biological samples and data for TOPMed.

Framingham Heart Study (phs000974)

WGS for "NHLBI TOPMed: Whole Genome Sequencing and Related Phenotypes in the Framingham Heart Study" (phs000974.v1.p1) was performed at the Broad Institute of MIT and Harvard (3R01HL092577-06S1, 3U54HG003067-12S2). We also acknowledge the dedication of the FHS study participants without whom this research would not be possible.

Jackson Heart Study (phs000964)

The Jackson Heart Study (JHS) is supported and conducted in collaboration with Jackson State University (HHSN268201800013I), Tougaloo College (HHSN268201800014I), the Mississippi State Department of Health (HHSN268201800015I) and the University of Mississippi Medical Center (HHSN268201800010I, HHSN268201800011I and HHSN268201800012I) contracts from the National Heart, Lung, and Blood Institute (NHLBI) and the National Institute for Minority Health and Health Disparities (NIMHD). The authors also wish to thank the staff and participants of the JHS.

Multi-Ethnic Study of Atherosclerosis (phs001416)

MESA and the MESA SHARe projects are conducted and supported by the National Heart, Lung, and Blood Institute (NHLBI) in collaboration with MESA investigators. Support for MESA is provided by contracts 75N92020D00001, HHSN268201500003I, N01-HC-95159, 75N92020D00005, N01-HC-95160, 75N92020D00002, N01-HC-95161, 75N92020D00003, N01-HC-95162, 75N92020D00006, N01-HC-95163, 75N92020D00004, N01-HC-95164, 75N92020D00007, N01-HC-95165, N01-HC-95166, N01-HC-95167, N01-HC-95168, N01-HC-95169, UL1-TR-000040, UL1-TR-001079, and UL1-TR-001420. Also supported by the National Center for Advancing Translational Sciences, CTSI grant UL1TR001881, and the National Institute of Diabetes and Digestive and Kidney Disease Diabetes Research Center (DRC) grant DK063491 to the Southern California Diabetes Endocrinology Research Center. MESA Family is conducted and supported by the National Heart, Lung, and Blood Institute (NHLBI) in collaboration with MESA investigators. Support is provided by grants and contracts R01HL071051, R01HL071205, R01HL071250, R01HL071251, R01HL071258, R01HL071259, and by the National Center for Research Resources, Grant UL1RR033176.

Women's Health Initiative (phs001237)

Author Manuscript

This article is protected by copyright. All rights reserved

The WHI program is funded by the National Heart, Lung, and Blood Institute, National Institutes of Health, U.S. Department of Health and Human Services through contracts HHSN268201600018C, HHSN268201600001C, HHSN268201600002C, HHSN268201600003C, and HHSN268201600004C.

We thank Tiffany Eulalio for her assistance in creating the graphical abstract. The graphical abstract contains images from BioRender.com.

D.N. is supported by 1T32AG047126-01. S.J. is supported by the Burroughs Wellcome Foundation Career Award for Medical Scientists, Foundation Leducq, Ludwig Center for Cancer Stem Cell Research, the American Society of Hematology Scholar Award, and the NIH Director's New Innovator Award (DP2-HL157540). We would like to thank Erik Bao for sharing his LD reference panel and Riccardo Marioni for his assistance in obtaining GWAS summary statistics for epigenetic age acceleration.

The views expressed in this manuscript are those of the authors and do not necessarily represent the views of the National Heart, Lung, and Blood Institute; the National Institutes of Health; or the U.S. Department of Health and Human Services.

A link to the full TOPMed Banner Authorship list can be found here: (https://www.nhlbiwgs.org/topmed-banner-authorship).

Conflicts of Interest

S. Jaiswal is a scientific advisor to Novartis, Roche Genentech, and Foresite Labs. UC Regents (the employer of S.Horvath and A.Lu) has filed patents surrounding several epigenetic biomarkers of aging (including GrimAge) which list S. Horvath and A. Lu as inventors. P. Natarajan reports grants support from Amgen, Apple, and Boston Scientific, and is a scientific advisor to Apple. S. Kathiresan is an employee of Verve Therapeutics, and holds equity in Verve Therapeutics, Maze Therapeutics, Catabasis, and San Therapeutics. He is a member of the scientific advisory boards for Regeneron Genetics Center and Corvidia Therapeutics; he has served as a consultant for Acceleron, Eli Lilly, Novartis, Merck, Novo Nordisk, Novo Ventures, Ionis, Alnylam, Aegerion, Haug Partners, Noble Insights, Leerink Partners, Bayer Healthcare, Illumina, Color Genomics, MedGenome, Quest, and Medscape. G. Abecasis is an employee of Regeneron Pharmaceuticals and owns stock and stock options for Regeneron Pharmaceuticals. S. Jaiswal and S. Kathiresan have jointly filed patents relating to clonal hematopoiesis and atherosclerotic cardiovascular disease.

Data Availability

Author Manuscript

This article is protected by copyright. All rights reserved

524 The data that support the findings of this study are available from Trans-Omics for Precision Medicine
525 (TOPMed) consortium. Restrictions apply to the availability of these data, which were used under license for
526 this study. Data are available at https://www.nhlbiwgs.org/topmed-data-access-scientific-community with the
527 permission of TOPMed Data Coordinating Center. All data used in the study is available at the follow DbGaP
528 accessions: Framingham Heart Study (phs000974.v1.p1), Jackson Heart Study (phs000964.v4.p1), Women's
529 Health Initiative (phs001237.v2.p1), Multi-ethnic Study of Atherosclerosis (phs000209.v13.p3).
530

531 **Author Contributions**

532 DN and SJ performed all statistical analyses and writing of the manuscript and DN created all figures and
533 tables. DN, SJ, AL, AB, JW, CK, TA, AP, JGW, and SH contributed to the study design and interpretation of
534 results. AL, AB, JEM, PD, CK, AR, JGW, and SH provided feedback on the writing of the manuscript. AL, AB,
535 PN, JW, MS, SK, GA, KT, XG, RT, PD, YL, CJ, SR, DVDB, CL, TB, GP, AC, LR, AJ, JM, JEM, PD, CK, TA,
536 DL, JR, AR, EW, JGW, and SH contributed to data acquisition and processing.

537 **References**

538 Bick AG, Pirruccello JP, Griffin GK, Gupta N, Gabriel S, Saleheen D, Libby P, Kathiresan S, & Natarajan P
539 (2020) Genetic Interleukin 6 Signaling Deficiency Attenuates Cardiovascular Risk in Clonal
540 Hematopoiesis. *Circulation* 141, 124–131.

541 Bick AG, Weinstock JS, Nandakumar SK, Fulco CP, Bao EL, Zekavat SM, Szeto MD, Liao X, Leventhal MJ,
542 Nasser J, Chang K, Laurie C, Burugula BB, Gibson CJ, Lin AE, Taub MA, Aguet F, Ardlie K, Mitchell
543 BD, Barnes KC, Moscati A, Fornage M, Redline S, Psaty BM, Silverman EK, Weiss ST, Palmer ND,
544 Vasan RS, Burchard EG, Kardia SLR, He J, Kaplan RC, Smith NL, Arnett DK, Schwartz DA, Correa A,
545 Andrade M de, Guo X, Konkle BA, Custer B, Peralta JM, Gui H, Meyers DA, McGarvey ST, Chen IY-D,
546 Shoemaker MB, Peyser PA, Broome JG, Gogarten SM, Wang FF, Wong Q, Montasser ME, Daya M,
547 Kenny EE, North KE, Launer LJ, Cade BE, Bis JC, Cho MH, Lasky-Su J, Bowden DW, Cupples LA,
548 Mak ACY, Becker LC, Smith JA, Kelly TN, Aslibekyan S, Heckbert SR, Tiwari HK, Yang IV, Heit JA,
549 Lubitz SA, Johnsen JM, Curran JE, Wenzel SE, Weeks DE, Rao DC, Darbar D, Moon J-Y, Tracy RP,
550 Buth EJ, Rafaels N, Loos RJF, Durda P, Liu Y, Hou L, Lee J, Kachroo P, Freedman BI, Levy D, Bielak
551 LF, Hixson JE, Floyd JS, Whitsel EA, Ellinor PT, Irvin MR, Fingerlin TE, Raffield LM, Armasu SM,
552 Wheeler MM, Sabino EC, Blangero J, Williams LK, Levy BD, Sheu WH-H, Roden DM, Boerwinkle E,
553 Manson JE, Mathias RA, Desai P, Taylor KD, Johnson AD, Auer PL, Kooperberg C, Laurie CC,
554 Blackwell TW, Smith AV, Zhao H, Lange E, Lange L, Rich SS, Rotter JI, Wilson JG, Scheet P, Kitzman
555 JO, Lander ES, Engreitz JM, Ebert BL, Reiner AP, Jaiswal S, Abecasis G, Sankaran VG, Kathiresan S
556 & Natarajan P (2020) Inherited causes of clonal haematopoiesis in 97,691 whole genomes. *Nature* 586,
557 763–768.

This article is protected by copyright. All rights reserved

Author Manuscript

558 Bild DE (2002) Multi-Ethnic Study of Atherosclerosis: Objectives and Design. *American Journal of*
559 *Epidemiology* 156, 871–881.

560 Blokzijl F, de Ligt J, Jager M, Sasselli V, Roerink S, Sasaki N, Huch M, Boymans S, Kuijk E, Prins P, Nijman IJ,
561 Martincorena I, Mokry M, Wiegerinck CL, Middendorp S, Sato T, Schwank G, Nieuwenhuis EES,
562 Verstegen MMA, van der Laan LJW, de Jonge J, IJzermans JNM, Vries RG, van de Wetering M,
563 Stratton MR, Clevers H, Cuppen E & van Boxtel R (2016) Tissue-specific mutation accumulation in
564 human adult stem cells during life. *Nature* 538, 260–264.

565 Bolton KL, Ptashkin RN, Gao T, Braunstein L, Devlin SM, Kelly D, Patel M, Berthon A, Syed A, Yabe M,
566 Coombs CC, Caltabellotta NM, Walsh M, Offit K, Stadler Z, Mandelker D, Schulman J, Patel A, Philip J,
567 Bernard E, Gundem G, Ossa JEA, Levine M, Martinez JSM, Farnoud N, Glodzik D, Li S, Robson ME,
568 Lee C, Pharoah PDP, Stopsack KH, Spitzer B, Mantha S, Fagin J, Boucai L, Gibson CJ, Ebert BL,
569 Young AL, Druley T, Takahashi K, Gillis N, Ball M, Padron E, Hyman DM, Baselga J, Norton L, Gardos
570 S, Klimek VM, Scher H, Bajorin D, Paraiso E, Benayed R, Arcila ME, Ladanyi M, Solit DB, Berger MF,
571 Tallman M, Garcia-Closas M, Chatterjee N, Diaz LA, Levine RL, Morton LM, Zehir A & Papaemmanuil
572 E (2020) Cancer therapy shapes the fitness landscape of clonal hematopoiesis. *Nature Genetics* 52,
573 1219–1226.

574 Carroll JE, Irwin MR, Levine M, Seeman TE, Absher D, Assimes T & Horvath S (2017) Epigenetic Aging and
575 Immune Senescence in Women With Insomnia Symptoms: Findings From the Women's Health
576 Initiative Study. *Biological Psychiatry* 81, 136–144.

577 Chen BH, Marioni RE, Colicino E, Peters MJ, Ward-Caviness CK, Tsai P-C, Roetker NS, Just AC, Demerath
578 EW, Guan W, Bressler J, Fornage M, Studenski S, Vandiver AR, Moore AZ, Tanaka T, Kiel DP, Liang
579 L, Vokonas P, Schwartz J, Lunetta KL, Murabito JM, Bandinelli S, Hernandez DG, Melzer D, Nalls M,
580 Pilling LC, Price TR, Singleton AB, Gieger C, Holle R, Kretschmer A, Kronenberg F, Kunze S, Linseisen
581 J, Meisinger C, Rathmann W, Waldenberger M, Visscher PM, Shah S, Wray NR, McRae AF, Franco
582 OH, Hofman A, Uitterlinden AG, Absher D, Assimes T, Levine ME, Lu AT, Tsao PS, Hou L, Manson JE,
583 Carty CL, LaCroix AZ, Reiner AP, Spector TD, Feinberg AP, Levy D, Baccarelli A, van Meurs J, Bell JT,
584 Peters A, Deary IJ, Pankow JS, Ferrucci L & Horvath S (2016) DNA methylation-based measures of
585 biological age: meta-analysis predicting time to death. *aging* 8, 1844–1865.

586 Christiansen L, Lenart A, Tan Q, Vaupel JW, Aviv A, McGue M & Christensen K (2016) DNA methylation age
587 is associated with mortality in a longitudinal Danish twin study. *Aging Cell* 15, 149–154.

588 Feinleib M, Kannel WB, Garrison RJ, McNamara PM & Castelli WP (1975) The framingham offspring study.
589 Design and preliminary data. *Preventive Medicine* 4, 518–525.
This article is protected by copyright. All rights reserved
Author Manuscript

590 Fuster JJ, MacLauchlan S, Zuriaga MA, Polackal MN, Ostriker AC, Chakraborty R, Wu C-L, Sano S,
591 Muralidharan S, Rius C, Vuong J, Jacob S, Muralidhar V, Robertson AAB, Cooper MA, Andrés V,
592 Hirschi KK, Martin KA & Walsh K (2017) Clonal hematopoiesis associated with TET2 deficiency
593 accelerates atherosclerosis development in mice. *Science* 355, 842–847.

594 Greenberg PL, Tuechler H, Schanz J, Sanz G, Garcia-Manero G, Solé F, Bennett JM, Bowen D, Fenaux P,
595 Dreyfus F, Kantarjian H, Kuendgen A, Levis A, Malcovati L, Cazzola M, Cermak J, Fonatsch C, Le
596 Beau MM, Slovak ML, Krieger O, Luebbert M, Maciejewski J, Magalhaes SMM, Miyazaki Y,
597 Pfeilstöcker M, Sekeres M, Sperr WR, Stauder R, Tauro S, Valent P, Vallespi T, van de Loosdrecht AA,
598 Germing U & Haase D (2012) Revised International Prognostic Scoring System for Myelodysplastic
599 Syndromes. *Blood* 120, 2454–2465.

600 Hannum G, Guinney J, Zhao L, Zhang L, Hughes G, Sadda S, Klotzle B, Bibikova M, Fan J-B, Gao Y,
601 Deconde R, Chen M, Rajapakse I, Friend S, Ideker T & Zhang K (2013) Genome-wide methylation
602 profiles reveal quantitative views of human aging rates. *Mol. Cell* 49, 359–367.

603 Hoang ML, Kinde I, Tomasetti C, McMahon KW, Rosenquist TA, Grollman AP, Kinzler KW, Vogelstein B &
604 Papadopoulos N (2016) Genome-wide quantification of rare somatic mutations in normal human
605 tissues using massively parallel sequencing. *Proc Natl Acad Sci USA* 113, 9846–9851.

606 Horvath S (2013) DNA methylation age of human tissues and cell types. *Genome Biology* 14, R115.

607 Horvath S (2011) *Weighted Network Analysis*, New York, NY: Springer New York. Available at:
608 http://link.springer.com/10.1007/978-1-4419-8819-5 [Accessed March 9, 2020].

609 Horvath S, Gurven M, Levine ME, Trumble BC, Kaplan H, Allayee H, Ritz BR, Chen B, Lu AT, Rickabaugh TM,
610 Jamieson BD, Sun D, Li S, Chen W, Quintana-Murci L, Fagny M, Kobor MS, Tsao PS, Reiner AP,
611 Edlefsen KL, Absher D & Assimes TL (2016) An epigenetic clock analysis of race/ethnicity, sex, and
612 coronary heart disease. *Genome Biol.* 17, 171.

613 Horvath S, Oshima J, Martin GM, Lu AT, Quach A, Cohen H, Felton S, Matsuyama M, Lowe D, Kabacik S,
614 Wilson JG, Reiner AP, Maierhofer A, Flunkert J, Aviv A, Hou L, Baccarelli AA, Li Y, Stewart JD, Whitsel
615 EA, Ferrucci L, Matsuyama S & Raj K (2018) Epigenetic clock for skin and blood cells applied to
616 Hutchinson Gilford Progeria Syndrome and *ex vivo* studies. *aging* 10, 1758–1775.

617 Horvath S & Raj K (2018) DNA methylation-based biomarkers and the epigenetic clock theory of ageing.
618 *Nature Reviews Genetics* 19, 371–384.

Author Manuscript

This article is protected by copyright. All rights reserved

619 Houseman EA, Accomando WP, Koestler DC, Christensen BC, Marsit CJ, Nelson HH, Wiencke JK & Kelsey
620 KT (2012) DNA methylation arrays as surrogate measures of cell mixture distribution. *BMC*
621 *Bioinformatics* 13, 86.

622 Jaiswal S & Ebert BL (2019) Clonal hematopoiesis in human aging and disease. *Science* 366, eaan4673.

623 Jaiswal S, Fontanillas P, Flannick J, Manning A, Grauman PV, Mar BG, Lindsley RC, Mermel CH, Burtt N,
624 Chavez A, Higgins JM, Moltchanov V, Kuo FC, Kluk MJ, Henderson B, Kinnunen L, Koistinen HA,
625 Ladenvall C, Getz G, Correa A, Banahan BF, Gabriel S, Kathiresan S, Stringham HM, McCarthy MI,
626 Boehnke M, Tuomilehto J, Haiman C, Groop L, Atzmon G, Wilson JG, Neuberg D, Altshuler D & Ebert
627 BL (2014) Age-Related Clonal Hematopoiesis Associated with Adverse Outcomes. *N Engl J Med* 371,
628 2488–2498.

629 Jaiswal S, Natarajan P, Silver AJ, Gibson CJ, Bick AG, Shvartz E, McConkey M, Gupta N, Gabriel S, Ardissino
630 D, Baber U, Mehran R, Fuster V, Danesh J, Frossard P, Saleheen D, Melander O, Sukhova GK,
631 Neuberg D, Libby P, Kathiresan S & Ebert BL (2017) Clonal Hematopoiesis and Risk of Atherosclerotic
632 Cardiovascular Disease. *N Engl J Med* 377, 111–121.

633 Levine ME, Lu AT, Quach A, Chen BH, Assimes TL, Bandinelli S, Hou L, Baccarelli AA, Stewart JD, Li Y,
634 Whitsel EA, Wilson JG, Reiner AP, Aviv A, Lohman K, Liu Y, Ferrucci L & Horvath S (2018) An
635 epigenetic biomarker of aging for lifespan and healthspan. *Aging (Albany NY)* 10, 573–591.

636 Lu AT, Quach A, Wilson JG, Reiner AP, Aviv A, Raj K, Hou L, Baccarelli AA, Li Y, Stewart JD, Whitsel EA,
637 Assimes TL, Ferrucci L & Horvath S (2019) DNA methylation GrimAge strongly predicts lifespan and
638 healthspan. *aging* 11, 303–327.

639 Lu AT, Seeboth A, Tsai P-C, Sun D, Quach A, Reiner AP, Kooperberg C, Ferrucci L, Hou L, Baccarelli AA, Li
640 Y, Harris SE, Corley J, Taylor A, Deary IJ, Stewart JD, Whitsel EA, Assimes TL, Chen W, Li S, Mangino
641 M, Bell JT, Wilson JG, Aviv A, Marioni RE, Raj K & Horvath S (2019) DNA methylation-based estimator
642 of telomere length. *Aging* 11. Available at: http://www.aging-
643 us.com/article/102173/text?_escaped_fragment_= [Accessed March 9, 2020].

644 Lu AT, Xue L, Salfati EL, Chen BH, Ferrucci L, Levy D, Joehanes R, Murabito JM, Kiel DP, Tsai P-C, Yet I, Bell
645 JT, Mangino M, Tanaka T, McRae AF, Marioni RE, Visscher PM, Wray NR, Deary IJ, Levine ME,
646 Quach A, Assimes T, Tsao PS, Absher D, Stewart JD, Li Y, Reiner AP, Hou L, Baccarelli AA, Whitsel
647 EA, Aviv A, Cardona A, Day FR, Wareham NJ, Perry JRB, Ong KK, Raj K, Lunetta KL & Horvath S
648 (2018) GWAS of epigenetic aging rates in blood reveals a critical role for TERT. *Nat Commun* 9, 387.

Author Manuscript

This article is protected by copyright. All rights reserved

649 Marioni RE, Shah S, McRae AF, Chen BH, Colicino E, Harris SE, Gibson J, Henders AK, Redmond P, Cox
650 SR, Pattie A, Corley J, Murphy L, Martin NG, Montgomery GW, Feinberg AP, Fallin MD, Multhaup ML,
651 Jaffe AE, Joehanes R, Schwartz J, Just AC, Lunetta KL, Murabito JM, Starr JM, Horvath S, Baccarelli
652 AA, Levy D, Visscher PM, Wray NR & Deary IJ (2015a) DNA methylation age of blood predicts all-
653 cause mortality in later life. *Genome Biol* 16, 25.

654 Marioni RE, Shah S, McRae AF, Chen BH, Colicino E, Harris SE, Gibson J, Henders AK, Redmond P, Cox
655 SR, Pattie A, Corley J, Murphy L, Martin NG, Montgomery GW, Feinberg AP, Fallin MD, Multhaup ML,
656 Jaffe AE, Joehanes R, Schwartz J, Just AC, Lunetta KL, Murabito JM, Starr JM, Horvath S, Baccarelli
657 AA, Levy D, Visscher PM, Wray NR & Deary IJ (2015b) DNA methylation age of blood predicts all-
658 cause mortality in later life. *Genome Biology* 16, 25.

659 Martincorena I & Campbell PJ (2015) Somatic mutation in cancer and normal cells. *Science* 349, 1483–1489.

660 Perna L, Zhang Y, Mons U, Holleczek B, Saum K-U & Brenner H (2016) Epigenetic age acceleration predicts
661 cancer, cardiovascular, and all-cause mortality in a German case cohort. *Clin Epigenetics* 8, 64.

662 Quach A, Levine ME, Tanaka T, Lu AT, Chen BH, Ferrucci L, Ritz B, Bandinelli S, Neuhouser ML, Beasley JM,
663 Snetselaar L, Wallace RB, Tsao PS, Absher D, Assimes TL, Stewart JD, Li Y, Hou L, Baccarelli AA,
664 Whitsel EA & Horvath S (2017) Epigenetic clock analysis of diet, exercise, education, and lifestyle
665 factors. *aging* 9, 419–446.

666 Ridker PM, Everett BM, Thuren T, MacFadyen JG, Chang WH, Ballantyne C, Fonseca F, Nicolau J, Koenig W,
667 Anker SD, Kastelein JJP, Cornel JH, Pais P, Pella D, Genest J, Cifkova R, Lorenzatti A, Forster T,
668 Kobalava Z, Vida-Simiti L, Flather M, Shimokawa H, Ogawa H, Dellborg M, Rossi PRF, Troquay RPT,
669 Libby P & Glynn RJ (2017) Antiinflammatory Therapy with Canakinumab for Atherosclerotic Disease. *N*
670 *Engl J Med* 377, 1119–1131.

671 Risques RA & Kennedy SR (2018) Aging and the rise of somatic cancer-associated mutations in normal
672 tissues S. M. Williams, ed. *PLoS Genet* 14, e1007108.

673 Ritchie ME, Phipson B, Wu D, Hu Y, Law CW, Shi W & Smyth GK (2015) limma powers differential expression
674 analyses for RNA-sequencing and microarray studies. *Nucleic Acids Research* 43, e47–e47.

675 Robertson NA, Hillary RF, McCartney DL, Terradas-Terradas M, Higham J, Sproul D, Deary IJ, Kirschner K,
676 Marioni RE & Chandra T (2019) Age-related clonal haemopoiesis is associated with increased
677 epigenetic age. *Current Biology* 29, R786–R787.

Author Manuscript

This article is protected by copyright. All rights reserved

678 Sempos CT, Bild DE & Manolio TA (1999) Overview of the Jackson Heart Study: A Study of Cardiovascular
679 Diseases in African American Men and Women. *The American Journal of the Medical Sciences* 317,
680 142–146.

681 Welch JS, Ley TJ, Link DC, Miller CA, Larson DE, Koboldt DC, Wartman LD, Lamprecht TL, Liu F, Xia J,
682 Kandoth C, Fulton RS, McLellan MD, Dooling DJ, Wallis JW, Chen K, Harris CC, Schmidt HK, Kalicki-
683 Veizer JM, Lu C, Zhang Q, Lin L, O'Laughlin MD, McMichael JF, Delehaunty KD, Fulton LA, Magrini
684 VJ, McGrath SD, Demeter RT, Vickery TL, Hundal J, Cook LL, Swift GW, Reed JP, Alldredge PA, Wylie
685 TN, Walker JR, Watson MA, Heath SE, Shannon WD, Varghese N, Nagarajan R, Payton JE, Baty JD,
686 Kulkarni S, Klco JM, Tomasson MH, Westervelt P, Walter MJ, Graubert TA, DiPersio JF, Ding L, Mardis
687 ER & Wilson RK (2012) The Origin and Evolution of Mutations in Acute Myeloid Leukemia. *Cell* 150,
688 264–278.

689 Wolf EJ, Maniates H, Nugent N, Maihofer AX, Armstrong D, Ratanatharathorn A, Ashley-Koch AE, Garrett M,
690 Kimbrel NA, Lori A, VA Mid-Atlantic MIRECC Workgroup, Aiello AE, Baker DG, Beckham JC, Boks MP,
691 Galea S, Geuze E, Hauser MA, Kessler RC, Koenen KC, Miller MW, Ressler KJ, Risbrough V, Rutten
692 BPF, Stein MB, Ursano RJ, Vermetten E, Vinkers CH, Uddin M, Smith AK, Nievergelt CM & Logue MW
693 (2018) Traumatic stress and accelerated DNA methylation age: A meta-analysis.
694 *Psychoneuroendocrinology* 92, 123–134.

695 Zink F, Stacey SN, Norddahl GL, Frigge ML, Magnusson OT, Jonsdottir I, Thorgeirsson TE, Sigurdsson A,
696 Gudjonsson SA, Gudmundsson J, Jonasson JG, Tryggvadottir L, Jonsson T, Helgason A, Gylfason A,
697 Sulem P, Rafnar T, Thorsteinsdottir U, Gudbjartsson DF, Masson G, Kong A & Stefansson K (2017)
698 Clonal hematopoiesis, with and without candidate driver mutations, is common in the elderly. *Blood*
699 130, 742–752.

700

701

702 **Figure Legends**

703 **Table 1. Summary of epigenetic clocks used in study.** IEAA = intrinsic epigenetic age acceleration, EEAA
704 = extrinsic epigenetic age acceleration.

705 **Figure 1**. **CHIP is associated with increased age acceleration.** Forest plot of the effect sizes and
706 confidence intervals for the effect of CHIP on age acceleration estimate from seven methylation clocks.

707 **Table 2. CHIP mutations in specific classes of genes have largely consistent effects on age**
708 **acceleration.** Table with effect sizes, standard errors and p-values for eight different classes of CHIP
709 mutations. "Multiple" means mutations in multiple genes. "DDR" refers to mutations in the DNA damage
710 response genes *TP53*, *PPM1D*, and *BRCC3*. "Splicing factor" are mutations in *SF3B1*, *SRSF2*, *U2AF1*,

This article is protected by copyright. All rights reserved

Author Manuscript

711 *ZRSR2*, and *PRPF8*. “Other” refers to mutations in all other genes not listed.

712 **Figure 2. CHIP and epigenetic age acceleration identify persons at high risk of all-cause mortality and 713 development of coronary heart disease (CHD).** **a** Scatterplot of correlation between AgeAccelGrim and 714 AgeAccelHannum in all cohorts. **b,c** Forest plots showing hazard ratios, confidence intervals and p-values for 715 Cox proportional hazard models of all-cause mortality (**b**) and development of CHD (**c**) in persons from FHS, 716 JHS, and WHI. All models included chronological age, race, low-density lipoprotein cholesterol, high-density 717 lipoprotein cholesterol, triglycerides, systolic blood pressure, type 2 diabetes status and smoking status as 718 covariates. Top two sections show the overall effect size of CHIP and age acceleration and bottom section 719 shows effect sizes based on dividing persons into four groups based upon presence of CHIP and age 720 acceleration. The results in **c** are a meta-analysis of events in FHS, JHS, WHI EMPC (unselected for CHD) 721 and WHI BA23 (case-control study for CHD). **d,e** Cumulative incidence plots of death (**d**) and CHD (**e**) in 722 persons divided into groups by presence of CHIP (CHIP+/CHIP-) and age acceleration 723 (AgeAccelHG+/AgeAccelHG-). The numbers in parentheses indicate the number of persons in each group for 724 these analyses. Only persons over 65 and free of CHD at baseline were used in **d** and **e**, while all persons 725 were used for **b** and **c**. **f** Cumulative incidence plot of death in persons with incident CHD after age 70. 726 Individuals who died less than 30 days after CHD were excluded.

727 **Figure S1. CHIP prevalence increases with age**. Plot of percentage of persons with CHIP as a function of 728 age divided in 5 year bins.

729 **Figure S2. CHIP carriers are older than controls.** Boxplot of age of persons with the different classes of 730 CHIP mutations.

731 **Figure S3. CHIP is associated with decreased methylation-estimated age-adjusted telomere length 732 (DNAmLTLAdjAge).** **a** Forest plot showing confidence intervals and p-values of association of all CHIP 733 mutations or specific classes of CHIP mutations with DNAmLTLAdjAge. **b** Box plots of DNAmLTLAdjAge as a 734 function of number of CHIP mutations. **c** Forest plot showing confidence intervals and p-values of correlation of 735 variant allele fraction (VAF) with DNAmLTLAdjAge.

736 **Figure S4. Methylation CpG sites used in clocks are hypomethylated in CHIP carriers. a,b** Volcano plots 737 from differential methylation analysis of persons with (**a**) *DNMT3A* and (**b**) *TET2* mutations vs. controls. The x-738 axis is the log fold change and the y-axis is the $-\log_{10}$ p-value for each CpG. **c** Scatter plot showing the 739 correlation of average M-values at CpGs shown in volcano plots in persons with *DNMT3A* and *TET2* 740 mutations.

741 **Figure S5. The risk of mortality and coronary heart disease (CHD) increases with CHIP in subjects with 742 age acceleration, and with age acceleration in subjects with CHIP, and is not affected by rs2228145 743 genotype or CRP levels.** **a,b** Forest plots showing hazard ratios, confidence intervals and p-values for 744 mortality (**a**) and development of CHD (**b**). The top section shows the effect of CHIP in subjects with age 745 acceleration, and the bottom section shows the effect of age acceleration in persons with CHIP. **c,d** Forest

Author Manuscript

This article is protected by copyright. All rights reserved

746 plots showing hazard ratios, confidence intervals and p-values as a function of CHIP status, age acceleration
747 and *IL6R* rs2228145 genotype for mortality (**c**) and development of CHD (**d**). Persons with at least 1 alternate
748 allele of rs2228145 were designated IL6RMut, and those with no alternate alleles were designated IL6RWT. **e,f**
749 Forest plots showing hazard ratios, confidence intervals and p-values as a function of CHIP status, age
750 acceleration and CRP levels for mortality (**e**) and development of CHD (**f**). Persons with greater than 2 mg/L of
751 CRP were designated CRPhi, and those with 2mg/L or less of CRP were designated CRPlo.
752 **Figure S6. rs2228145 reduces the increased risk in composite mortality/CHD cumulative risk in**
753 **persons with TET2 CHIP mutations and epigenetic age acceleration.** Forest plot showing hazard ratios,
754 confidence intervals and p-values for Cox proportional hazard models of the composite measure of
755 mortality/CHD risk in persons from FHS, JHS, and WHI AS315. Model includes chronological age, race, low-
756 density lipoprotein cholesterol, high-density lipoprotein cholesterol, triglycerides, systolic blood pressure, type 2
757 diabetes status and smoking status as covariates. IL6Mut = 1 or 2 copies of alternate allele for rs2228145,
758 IL6WT = 0 copies of alternate allele for rs2228145.
759 **Table S1. Demographics of cohorts used in study.** WHI = Women's Health Initiative, FHS = Framingham
760 Heart Study, JHS = Jackson Heart Study, MESA = Multiethnic Study of Atherosclerosis, AA = African
761 American, CHD = coronary heart disease. [1]WHI BA23 was excluded from the mortality analysis because it was
762 a case-control study for CHD. [2]WHI BA23 was analyzed for CHD risk separately from the other cohorts
763 becuase it was a case-control study for CHD. [3]MESA subjects were excluded from mortality and CHD analysis
764 because they were selected for survival over 10 years, which biased subject selection.
765 **Table S2. Increasing number of CHIP mutations is associated with increased age acceleration and**
766 **other methylation measures.** Tables with effect sizes, standard errors and p-values of the comparison of
767 persons with 2 CHIP mutations vs 1, and >2 mutations vs. 2 in (**a**) age acceleration in methylation clocks, (**b**)
768 DNAmGrimAge biomarkers, and (**c**) predicted cell type abundance.
769 **Table S3. CHIP mutations in specific classes of genes affect Grim biomarkers and predicted cell type**
770 **abundances.** Tables with effect sizes, standard errors and p-values of the association of CHIP mutations in
771 specific classes of genes with (**a**) DNAmGrimAge biomarkers and (**b**) predicted cell type abundance.
772 **Table S4. Variant allele fraction is correlated with some methylation measures.** Tables with correlation
773 coefficients, standard errors and p-values of the correlation of VAF in all CHIP carriers and in specific classes
774 of genes with (**a**) age acceleration in methylation clocks, (**b**) DNAmGrimAge biomarkers, and (**c**) predicted cell
775 type abundance.
776 **Table S5. The Hannum and Grim clocks interact with CHIP to increase risk of mortality.** Table with
777 hazard ratios, standard errors and p-values of Cox proportional hazard models for the interaction of CHIP and
778 epigenetic age acceleration with mortality for individual clocks.
779 **Table S6. Genes and variants queried for the assessment of CHIP.** Shown are gene names and reported
780 mutations in these genes that were used to classify persons as having clonal hematopoiesis.

Author Manuscript

This article is protected by copyright. All rights reserved

781 **Table S7. CHIP mutations identified in this analysis.** Each row is one person in the study. CHIP status is
782 given by “Has CHIP”. Also identified are mutated gene(s) (“Mutated Gene”), mutation type
783 (“ExonicFunc.refGene”), amino acid change (“NonsynOI”), variant allele fraction (“AF”), reference and alternate
784 allele (“REF”,”ALT”), and reference and alternate allele counts (“refcount”,”altcount”).

Author Manuscript

This article is protected by copyright. All rights reserved

Clock	Type	Tissue	Outcome	Publication	Notes
Horvath	Intrinsic	Multiple	Chronological age	Horvath 2013	Inaccessible tissues primarily from tissue-adjacent normal samples in The Cancer Genome Atlas (see publication).
IEAA	Intrinsic	Multiple	Chronological age	Quach et al. 2017	Uses same CpGs as Horvath clock, but reweighted as described in Quach et al. to minimize influence of cell composition.
Hannum	Extrinsic	Whole blood	Chronological age	Hannum 2013	Highly correlated with aging related changes in blood cell composition.
EEAA	Extrinsic	Whole blood	Chronological age	Quach et al. 2017	Uses same CpGs as Hannum clock, but reweighted as described in Quach et al. to maximize influence of cell composition.
SkinAndBloodClock	Intrinsic	Whole blood, fibroblasts	Chronological age	Horvath et al. 2018	Created to address poor age prediction in Horvath clock in skin and whole blood.
PhenoAge	Extrinsic	Whole blood	Time to death	Levine et al. 2018	PhenoAge is measure of mortality risk derived from National Health and Nutrition Examination Survey using the following markers: albumin, creatinine, serum glucose, log C-reactive protein, lymphocyte percent, mean red cell volume, red cell distribution width, alkaline phosphatase, white blood cell count, and age (see publication for details).
GrimAge	Extrinsic	Whole blood	Time to death	Lu et al. 2019	Methylation is used to predict 8 surrogate biomarkers: Adrenomedullin (ADM), Beta-2-Microglobulin (B2M), Cystatin C, Growth Differentiation Factor 15 (GDF15), Leptin, Serpin Family E Member 1 (SERPINE/PAI1), TIMP Metalloproteinase Inhibitor 1 (TIMP1), smoking pack years (PACKYRS). The predicted values of those biomarkers are used to predict mortality (see publication for details).

Author Manuscript

This article is protected by copyright. All rights reserved

Class	Horvath		IEAA		Hannum		EEAA		SkinBloodClock		PhenoAge		GrimAge	
	est. (SE)	p-value	est. (SE)	p-value	est. (SE)	p-value	est. (SE)	p-value	est. (SE)	p-value	est. (SE)	p-value	est. (SE)	p-value
All	3.01 (0.27)	3.0×10^{-25}	2.92 (0.26)	9.3×10^{-26}	2.71 (0.26)	1.8×10^{-23}	3.08 (0.33)	3.7×10^{-18}	1.58 (0.20)	2.5×10^{-13}	2.21 (0.36)	1.0×10^{-8}	1.31 (0.25)	8.6×10^{-7}
DNMT3A	2.58 (0.38)	2.2×10^{-10}	2.72 (0.36)	2.1×10^{-12}	1.76 (0.35)	5.7×10^{-6}	1.75 (0.46)	6.8×10^{-4}	1.44 (0.28)	1.8×10^{-6}	2.16 (0.51)	5.8×10^{-5}	0.61 (0.35)	0.123
TET2	2.58 (0.59)	4.8×10^{-5}	2.47 (0.57)	4.9×10^{-5}	3.86 (0.55)	2.1×10^{-11}	4.07 (0.72)	7.2×10^{-8}	0.91 (0.44)	0.060	1.31 (0.79)	0.135	0.99 (0.55)	0.093
Multiple	7.43 (0.93)	5.6×10^{-15}	6.77 (0.89)	1.1×10^{-13}	8.36 (0.86)	3.0×10^{-21}	10.97 (1.13)	2.5×10^{-21}	5.01 (0.69)	10.0×10^{-13}	6.35 (1.24)	5.3×10^{-7}	4.85 (0.85)	2.4×10^{-8}
DDR	0.21 (1.06)	0.962	-0.21 (1.01)	0.717	0.31 (0.98)	0.871	1.43 (1.29)	0.327	-0.26 (0.79)	0.660	0.63 (1.41)	0.718	-0.27 (0.97)	0.723
JAK2	3.80 (1.67)	0.029	1.37 (1.60)	0.448	5.88 (1.56)	2.3×10^{-4}	6.21 (2.04)	0.003	4.31 (1.24)	6.7×10^{-4}	10.01 (2.23)	9.7×10^{-6}	3.46 (1.54)	0.028
ASXL1/2	2.86 (1.06)	0.011	2.75 (1.01)	0.011	1.46 (0.98)	0.183	1.87 (1.29)	0.188	0.44 (0.79)	0.652	-0.55 (1.41)	0.634	3.11 (0.97)	0.002
Splicing factor	5.02 (1.57)	0.002	4.88 (1.51)	0.002	2.70 (1.47)	0.082	2.41 (1.92)	0.242	2.36 (1.17)	0.052	2.46 (2.11)	0.267	2.37 (1.45)	0.112
Other	4.20 (1.31)	0.002	4.40 (1.26)	7.3×10^{-4}	0.98 (1.22)	0.497	1.68 (1.60)	0.345	1.99 (0.97)	0.050	0.73 (1.75)	0.726	1.95 (1.21)	0.120

Author Manuscript
This article is protected by copyright. All rights reserved

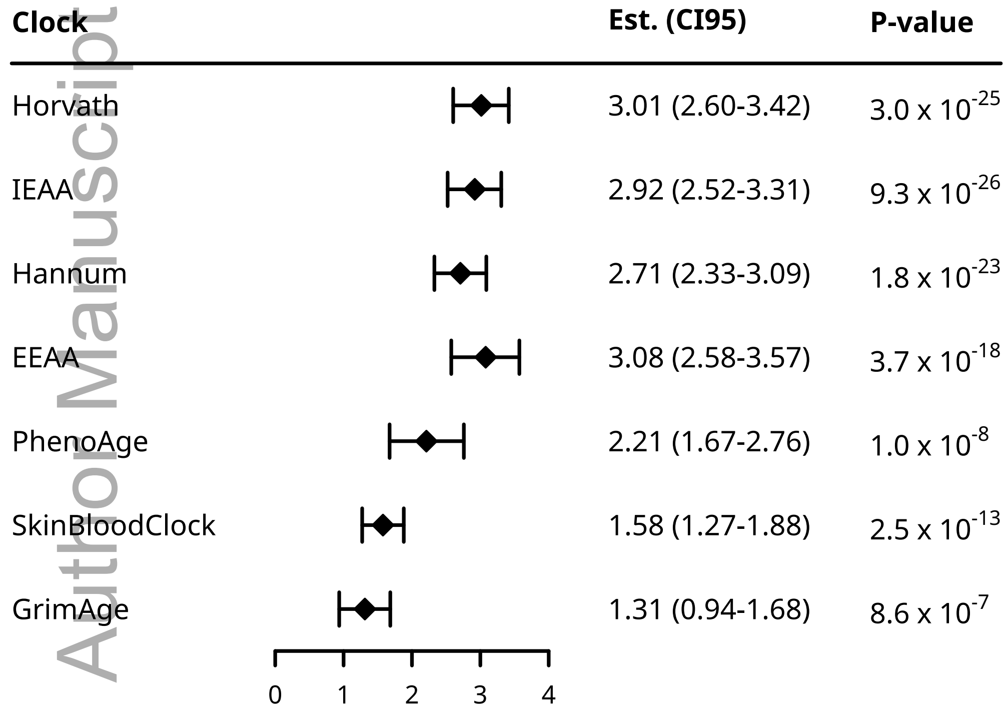

Author Manuscript

This article is protected by copyright. All rights reserved

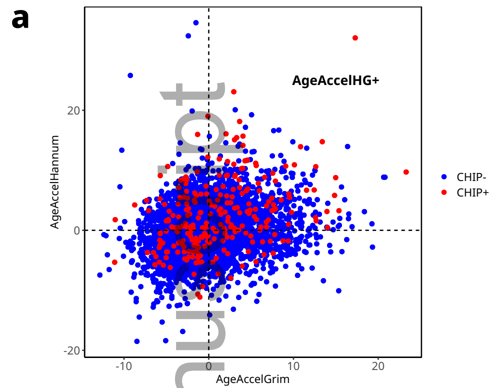

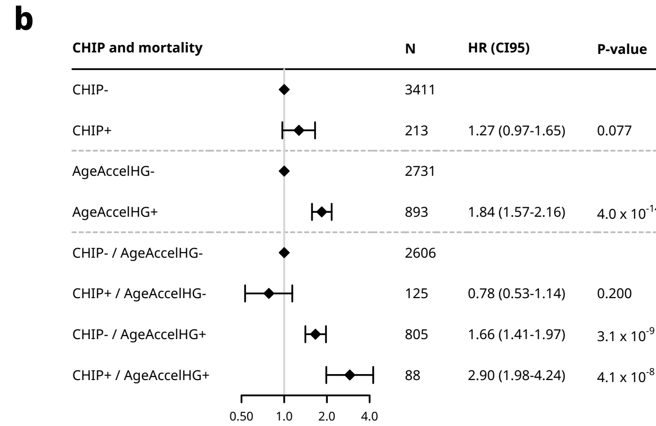

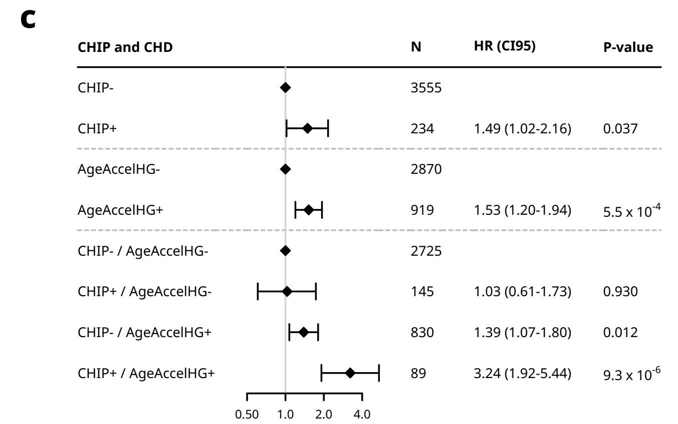

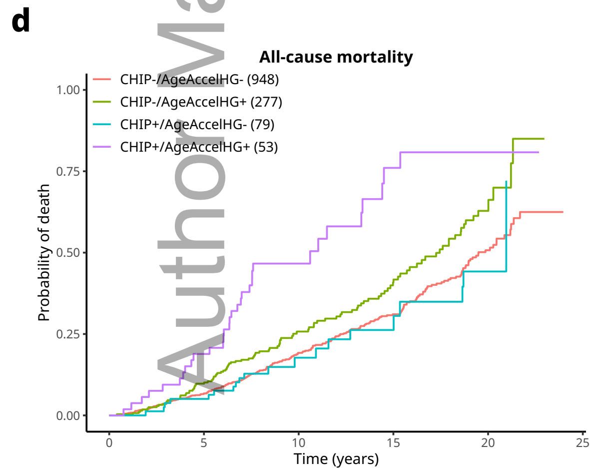

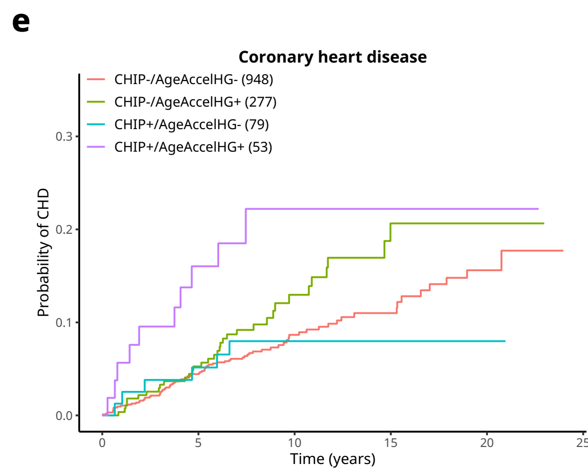

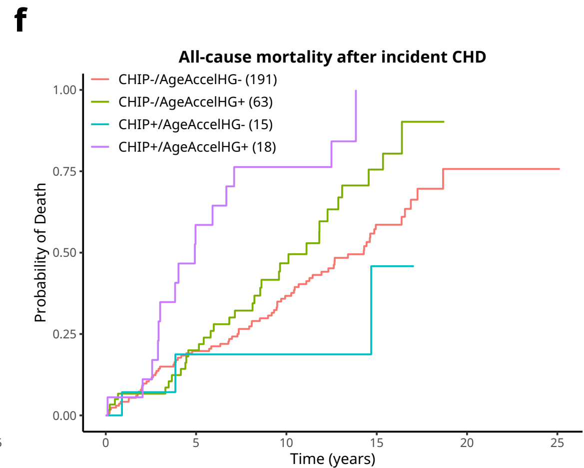

Author Manuscript

This article is protected by copyright. All rights reserved